ISSN 1674-1056
http://cpb.iphy.ac.cn
http://iopscience.iop.org/cpb
中国物理 B
Chinese Physics
中国物理
Chinese Physics B

Manipulation of acoustic wavefront by transmissive metasurface based on pentamode metamaterials

Ying Liu(刘颖), Yi-Feng Li(李义丰), Xiao-Zhou Liu(刘晓宙)

Citation: Chin. Phys. B . 2019, 28(2): 024301. **doi:** 10.1088/1674-1056/28/2/024301
Journal homepage: http://cpb.iphy.ac.cn; http://iopscience.iop.org/cpb

What follows is a list of articles you may be interested in

Theoretical prediction of the yield of strong oxides under acoustic cavitation

Jing Sun(孙晶), Zhuangzhi Shen(沈壮志), Runyang Mo(莫润阳)
Chin. Phys. B . 2019, 28(1): 014301. **doi:** 10.1088/1674-1056/28/1/014301

Bidirectional asymmetric acoustic focusing with two flat acoustic metasurfaces

Di-Chao Chen(陈帝超), Xing-Feng Zhu(朱兴凤), Qi Wei(魏琦), Da-Jian Wu(吴大建)
Chin. Phys. B . 2018, 27(12): 124302. **doi:** 10.1088/1674-1056/27/12/124302

Thermoacoustic-reflected focusing lens based on acoustic Bessel-like beam with phase manipulation

An-Ru Hou(侯安茹), Wen-Ting Gao(高文婷), Jiao Qian(钱姣), Hong-Xiang Sun(孙宏祥), Yong Ge(葛勇), Shou-Qi Yuan(袁寿其), Qiao-Rui Si(司乔瑞), Xiao-Jun Liu(刘晓峻)
Chin. Phys. B . 2018, 27(12): 124301. **doi:** 10.1088/1674-1056/27/12/124301

Influence of mode conversions in the skull on transcranial focused ultrasound and temperature fields utilizing the wave field separation method: A numerical study

Xiang-Da Wang(王祥达), Wei-Jun Lin(林伟军), Chang Su(苏畅), Xiu-Ming Wang(王秀明)
Chin. Phys. B . 2018, 27(2): 024302. **doi:** 10.1088/1674-1056/27/2/024302

Wavefront modulation of water surface wave by a metasurface

Sun Hai-Tao, Cheng Ying, Wang Jing-Shi, Liu Xiao-Jun
Chin. Phys. B . 2015, 24(10): 104302. **doi:** 10.1088/1674-1056/24/10/104302

Manipulation of acoustic wavefront by transmissive metasurface based on pentamode metamaterials*

Ying Liu(刘颖)[1], Yi-Feng Li(李义丰)[1,2,†], and Xiao-Zhou Liu(刘晓宙)[3]

[1] College of Computer Science and Technology, Nanjing Tech University, Nanjing 211800, China
[2] Key Laboratory of Modern Acoustics, Ministry of Education, Nanjing University, Nanjing 210093, China
[3] Key Laboratory of Modern Acoustics, Ministry of Education, Institute of Acoustics and School of Physics, Nanjing University, Nanjing 210093, China

(Received 12 October 2018; revised manuscript received 26 November 2018; published online 10 January 2019)

An underwater acoustic metasurface with sub-wavelength thickness is designed for acoustic wavefront manipulation. In this paper, a pentamode lattice and a frequency-independent generalized acoustic Snell's law are introduced to overcome the limitations of narrow bandwidth and low transmittance. The bulk modulus and effective density of each unit cell can be tuned simultaneously, which are modulated to guarantee the achievement of refractive index profile and high transmission. Here, we actualize anomalous refraction, generation of non-diffracting Bessel beam, sub-wavelength flat focusing, and surface wave conversion by constructing inhomogeneous acoustic metasurface. This design approach has potential applications in medical ultrasound imaging and underwater acoustic communications.

Keywords: metasurface, frequency-independent, pentamode, high transmission

PACS: 43.35.+d, 43.20.+g, 68.60.Bs **DOI:** 10.1088/1674-1056/28/2/024301

1. Introduction

Acoustic metasurfaces are one of the active domains in the study of acoustic metamaterial and has aroused many researchers' interest in the past few years.[1–10] The core idea of a metasurface is to introduce the required phase arrangement by placing the sub-wavelength structure at the interface between two natural materials. The well-designed phase distribution provides a new method to regulate the propagation of acoustic waves. Due to its planar, ultrathin physical structure and excellent capability of wavefront control, the acoustic metasurfaces have a wide range of potential applications, including anomalous scattering/refraction,[11,12] ultrathin focusing lens,[13,14] acoustic bend,[15–17] conversion of propagating waves into surface waves, and planar aberration-free lens.[18]

In addition, there is larger room for improvement because the time for studying the acoustic metasurface is relatively short. The practical application of conventional acoustic metasurface is often limited by three key factors. The first limitation is the low transmittance caused by the huge impedance mismatch between the metasurface and the background medium. In previous studies, acoustic metasurfaces are mostly constructed by simple labyrinth microstructural elements.[19–22] Although the structure of the unit is simple and easy to process, the relationship between the effective acoustic parameters and the structural parameters is complicated. In consequence the design of labyrinthine unit is mostly simplified, which only guarantees the requirement of gradient profile for abrupt phase but neglects the impedance matching. Another limitation is inherent narrow working bandwidth. According to the generalized acoustic Snell's law (GASL),[1] the correction term of the refraction angle/reflection angle is not only related to the transverse gradient variation of the metasurface but also to the incident wave frequency. An acoustic metasurface with gradient phase distribution based on this theory can only work at a selected single frequency and cannot achieve broadband acoustic effects. Finally, the last limitation is excessive metamaterial volume size. Since the wavelength of the acoustic wave in the audible range is too long, the requirement for miniaturization of the device has become more urgent. To solve these problems, a broadband pentamode material is introduced as a basic unit cell of the metasurface to realize broadband manipulation.[23–26] The pentamode material composed of metal has a relatively stable shape and its effective shear modulus is much smaller than its effective bulk modulus, which gives it similar acoustic properties to those in fluids. Moreover, the effective parameters of the pentamode material depend on the constitutive parameters and geometric construction of the material, and can be adjusted simultaneously.[26]

In this article, we use two-dimensional (2D) pentamode material (PM) lattice to design an underwater acoustic metasurface based on a frequency-independent GASL. Compared with a pentamode cell with additional weight unit at the vertex of a cell, the weight added at the midpoint enhances the bending resistance of the connecting rod and makes the ro-

*Project supported by the National Natural Science Foundation of China (Grant Nos. 61571222 and 11474160), the Natural Science Foundation of Jiangsu Province, China (Grant No. BK20161009), and the Six-Talent Peaks Project of Jiangsu Province, China.

†Corresponding author. E-mail: lyffz4637@163.com

© 2019 Chinese Physical Society and IOP Publishing Ltd

tation mode shift to high frequency.[27] Therefore, the PM in this paper has better underwater acoustic control effect and can be used in low frequency. The metasurface has a gradient refractive index and its acoustic impedance matches the background medium. In this proposal, we employ the transversal gradient index instead of gradient phase in the correction term, which has a broadband characteristic due to the lack of a frequency term. Moreover, a series of pentamode material elements with different refractive indices and impedance matching in a certain frequency band has been designed to fabricate the acoustic metasurface. In this work, the excellent wavefront manipulations are demonstrated, such as broadband and efficient anomalous refraction, generation of non-diffracting Bessel beam, sub-wavelength flat focusing and cylindrical-to-plane-wave conversion.

2. Theory of the acoustic metasurface

It is assumed that the sound wave of frequency f is incident from a medium with a sound velocity c_i to another with sound velocity c_t. At the boundary between the two media along the x axis, the ultrathin acoustic metasurface is artificially constructed to introduce an abrupt phase $\Phi(x)$, which changes continuously along the x direction. At this time, the generalized acoustic Snell's law can be expressed as

$$k_\mathrm{t}\sin\theta_\mathrm{t}-k_\mathrm{i}\sin\theta_\mathrm{i}=\frac{\mathrm{d}\Phi(x)}{\mathrm{d}x}, \tag{1}$$

where θ_i and θ_t are the angle of incidence and refraction, while k_i and k_t are the wavenumber of incident acoustic wave and refractive acoustic wave respectively ($k_\mathrm{i}=2\pi f/c_\mathrm{i}$,$k_\mathrm{t}=2\pi f/c_\mathrm{t}$). According to the GASL, the direction of the transmitted wave can be manipulated when the metasurface guarantees a suitable abrupt phase gradient. The integral of Eq. (1) can be obtained as

$$\Phi(x)=\int\left[k_\mathrm{t}\sin\theta_\mathrm{t}(x)-k_\mathrm{i}\sin\theta_\mathrm{i}(x)\right]\mathrm{d}x. \tag{2}$$

Hence, the phase accumulation across the metasurface can be obtained according to the desired refracted angle, incident angle and wave number on either side of the metasurface. Here, we consider the two simplified conditions, *i.e.*, the same homogeneous medium of both sides ($k_\mathrm{i}=k_\mathrm{t}=k_0$) and normal incidence ($\theta_\mathrm{i}=0$), then Eq. (2) can be simplified into

$$\Phi(x)=k_0\int\sin\theta_\mathrm{t}(x)\,\mathrm{d}x. \tag{3}$$

To broaden the working frequency range, the working mechanism of the broadband acoustic metasurface is discussed firstly. Figure 1(a) is a schematic diagram of the acoustic metasurface. The background medium of the upper side and the lower side of the metasurface are the same medium, the corresponding refractive index and the density are n_0 and ρ_0, respectively. The proposed metasurface with thickness t_m is distributed along the x axis, and the density $\rho(x)$ and refractive index $n(x)$ are in gradient distributions. The refractive index is defined as $n(x)=c_0/c(x)$, where $c(x)$ is the sound velocity distribution of the metasurface along the x direction. To match the acoustic impedance between the metasurface and the background medium, the following equation is required:

$$\rho(x)c(x)=\rho_0 c_0. \tag{4}$$

Due to impedance matching, when a plane wave of frequency f is normally incident on the surface along the $+y$ direction [$\theta_\mathrm{i}(x)=0$], the abrupt phase introduced by the metasurface is essentially a phase delay. The phase accumulation across the metasurface can be expressed as

$$\Phi(x)=\frac{2\pi f t_\mathrm{m}}{c(x)}=\frac{t_\mathrm{m}k_0c_0}{c(x)}=t_\mathrm{m}k_0n(x). \tag{5}$$

Substituting Eq. (5) and $\theta_\mathrm{i}(x)=0$ into Eq. (1), the refracted angle of the acoustic metasurface can be obtained as

$$\sin\theta_\mathrm{t}(x)=t_\mathrm{m}\frac{\mathrm{d}n(x)}{\mathrm{d}x}. \tag{6}$$

Equation (6) implies that the refracted angle is related to the refractive index gradient of the metasurface when the plane wave is incident perpendicularly. Therefore, the transmission direction of transmitted acoustic wave can be changed arbitrarily by appropriately adjusting the refractive index gradient of the metasurface. It is of note that equation (6) does not contain a frequency term, so the metasurface has a broadband acoustic wavefront manipulation function as long as the refractive index does not vary with frequency. According to Eqs. (6) and (4), the refractive index and density distribution of the broadband acoustic metasurface can be obtained as

$$n(x)=\frac{1}{t_\mathrm{m}}\int\sin\theta_\mathrm{t}(x)\,\mathrm{d}x, \tag{7}$$

$$\rho(x)=\rho_0 n(x). \tag{8}$$

Equation (7) relates the refractive index distribution to the desired acoustic wavefront manipulation, while equation (8) describes the relationship between the density and the refractive index to meet the requirement for impedance matching. Equations (7) and (8) together depict a basis theory for designing a broadband metasurface.

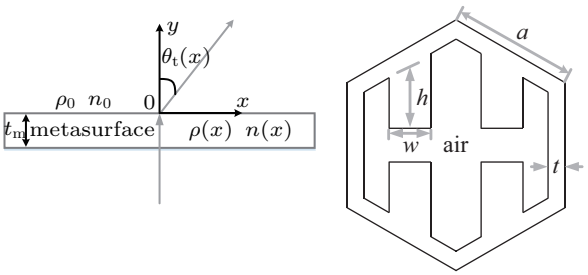


Fig. 1. (a) Schematic diagram of impedance matching acoustic metasurface and (b) illustration of hexagonal pentamode structure.

Table 1. Structural parameters and desired acoustic parameters for pentamode metamaterials.

	Structural parameters				Desired acoustic parameters		
	a/mm	t/mm	h/mm	w/mm	n'	B'	ρ'
U_1	3	0.57	0.455	0.37	1.1	$10\rho_0 c_0^2/11$	$1.1\rho_0$
U_2	3	0.45	1.715	1.36	1.7	$10\rho_0 c_0^2/17$	$1.7\rho_0$
U_3	3	0.36	0.82	0.35	2.3	$10\rho_0 c_0^2/23$	$2.3\rho_0$
U_4	3	0.33	1.51	0.6	2.9	$10\rho_0 c_0^2/29$	$2.9\rho_0$
U_5	3	0.3	1.555	1.01	3.5	$10\rho_0 c_0^2/35$	$3.5\rho_0$
U_6	3	0.55	1.495	0.28	4.1	$10\rho_0 c_0^2/41$	$4.1\rho_0$

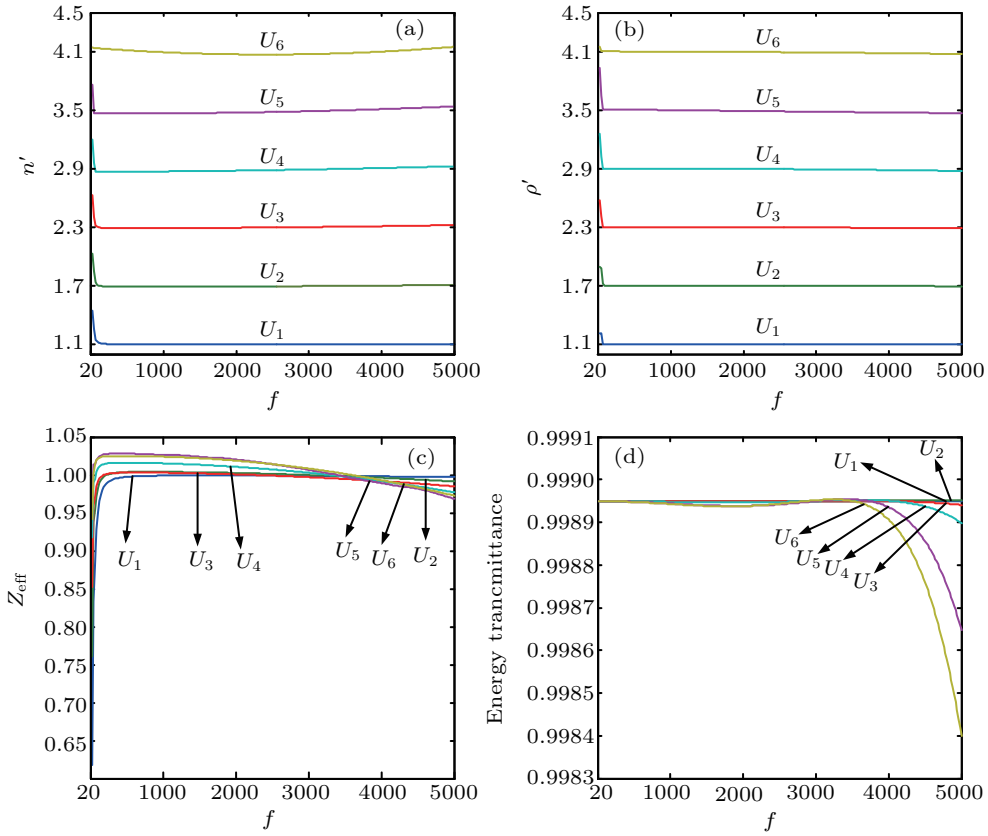


Fig. 2. Effective acoustic parameters of six pentamode units: (a) refractive index n', (b) effective density ρ', (c) effective acoustic impedance Z_{eff}; and (d) acoustic energy transmittance.

In this paper, six types of pentamode unit cells are designed to construct the proposed metasurface. The model of 2D PM is constructed as shown in Fig. 1(b). The unit cell structure is composed of a regular hexagonal lattice and additional weight units attached to the midpoint of the honeycomb wall. The side length and the width of the regular hexagon, and the length and the width of the additional weight are a, t, h, and w, respectively, as shown in Fig. 1(b). The interior of metal framework is filled with air and the background medium is water. Under the limitation of long wavelength, the effective density of the pentamode metamaterial is approximately equal to its volume average density, and its effective bulk modulus is determined by the geometric parameters of the unit and the acoustic parameters of the metal framework.[24,28] Therefore, the pentamode material exhibits non-dispersive characteristics in a certain low frequency range and the effective refractive index does not vary with frequency. We design these six pentamode units denoted as U_1 to U_6 to fabricate the impedance matching broadband metasurface. The values of desired effective refractive index $n' = c_0/c'$ for these units are designed in a range from 1.1 to 4.1 in steps of 0.6. To match the impedance of background medium, the effective density ρ' and effective sound velocity c' should satisfy $\rho' c' = \rho_0 c_0$, and then the effective bulk modulus and the density of each unit can be acquired as

$$B' = \rho_0 c_0^2/n', \tag{9}$$

$$\rho' = \rho_0 n'. \tag{10}$$

As described by Eqs. (9) and (10), the desired effective bulk modulus and effective density of pentamode units can be obtained. The detailed structural parameters and effective acoustic parameters are listed in Table 1. Based on the finite element method (FEM),[29] the transmission coefficient and reflection coefficient of the pentamode unit can be calculated, and the effective acoustic parameters of the six units can be obtained by the retrieval method[30] as shown in Figs. 2(a)–2(d). Figures 2(a) and 2(b) show that the effective refractive index and effective density of each unit meet their target values. Figure 2(c) illustrates that the equivalent relative impedance of each unit is approximately equal to 1 in the working frequency range, indicating that each cell and background medium are impedance matched. Figure 2(d) is a diagram showing the change of sound energy transmittance with acoustic frequency. It is found that the transmittance of each unit is higher than 95% in the investigated frequency band, which proves that these units are highly transparent to sound waves.

3. Simulation results

In this section, pentamode material units are used to construct a broadband acoustic metasurface to manipulate the sound waves for realizing efficient anomalous acoustic refraction, Bessel beam generation, and acoustic focusing.

First, we demonstrate the realization of broadband anomalous acoustic refraction by using the designed metasurfaces. As shown in Fig. 3(a), the plane wave is incident vertically on the acoustic metasurface and deflects after passing through the metasurface, which leads to the anomalous refraction. If the refraction angle is a constant θ_1 with respect to the x direction, then $\theta_t(x) = \theta_1$ is taken in Eq. (7). The refractive index distribution $n_1(x)$ of the ideal acoustic metasurface can be expressed as $n_1(x) = x\sin\theta_1/t_m + C_1$, where C_1 is an arbitrary constant obtained by integration. The black dotted line in Fig. 3(b) represents the distribution of the refractive index of the ideal metasurface along the x direction when setting $\theta_1 = 15.5^\circ$ and $C_1 = 4/5$. The red solid line in the figure refers to the gradient profile of the metasurface horizontal direction designed in this paper. According to Eq. (6), refraction angle is proportional to the thickness t_m and the gradient refractive index of the metasurface. Consequently, a seven-layer pentamode material unit ($t_m = 7t$) is used to construct the metasurface and expand the control range of the refraction angle due to the fact that the designed pentamode material provides only six finite refractive index values. The gaps between adjacent layers are filled with background medium. Even with a seven-layer pentamode material unit, the thickness of the metasurface is still sub-wavelength in the whole working frequency range. In order to verify the generation of anomalous refraction phenomenon, the acoustic pressure field distribution is calculated based on the FEM simulation. Figures 3(c) and 3(d) illustrate the acoustic pressure field distribution of the plane Gaussian acoustic beam incident on a pentamode metasurface with frequency $f = 3500$ Hz and $f = 5000$ Hz, respectively. Obvious anomalous acoustic refraction can be found. The transmitted acoustic wave in the region above the metasurface still maintains a planar Gaussian shape, but the propagation direction is significantly deflected in comparison with the incident direction, and the propagation direction of the transmitted wave conforms to the theoretical prediction direction (black arrow). Considering the working band (3500 Hz$< f <$ 5000 Hz), the relationship between refracted angle and incident acoustic frequency is shown in Fig. 3(e). It can be found that the simulated refracted angle (circle) is basically consistent with the theoretical angle (dotted line) throughout the studied frequency band.

Figure 4(a) shows a schematic diagram of a Bessel beam generation based on broadband metasurface. Since the Bessel beam can be superimposed by two plane waves with opposite propagation angles, the superimposed region is the Bessel beam generation region. Therefore, the transmitted wave beam should be divided into two columns of refracting plane waves with angles of refraction $\pm\theta_2$ ($\theta_t = -\theta_2 x/|x|$). According to Eq. (3), the refractive index distribution $n_2(x)$ of the ideal acoustic metasurface for generating Bessel beam is $n_2(x) = -|x|\sin\theta_2/t_m + C_2$, where C_2 is an arbitrary constant obtained by integration. The black dotted line in Fig. 4(b) represents the refractive index distribution of the ideal metasurface along the x direction when $\theta_2 = 15.5^\circ$ and $C_2 = 22/5$. It can be found that the refractive index of the ideal metasurface is symmetrically distributed with respect to $x = 0$ and increases linearly with x. The discrete metasurface refractive index distribution is also plotted in Fig. 4(b) (solid red line). Based on the FEM simulation, the acoustic energy distribution of the pentamode metasurface is calculated to verify the effect of the non-diffracting Bessel beams generated by the broadband pentamode metasurface. When a plane acoustic beam with the frequency $f = 5000$ Hz is perpendicularly incident on the pentamode metasurface, the acoustic intensity field distribution is shown in Fig. 4(c), and the transmitted acoustic waves in the region above the metasurface are almost within the theoretically predicted Bessel beam generation region (shown in the black wireframe). The generated acoustic waves travel along a straight line, the energy is concentrated near the axial direction, and the acoustic beam energy does not diverge within a considerable distance. These characteristics are consistent with the characteristics of the acoustic Bessel beam.

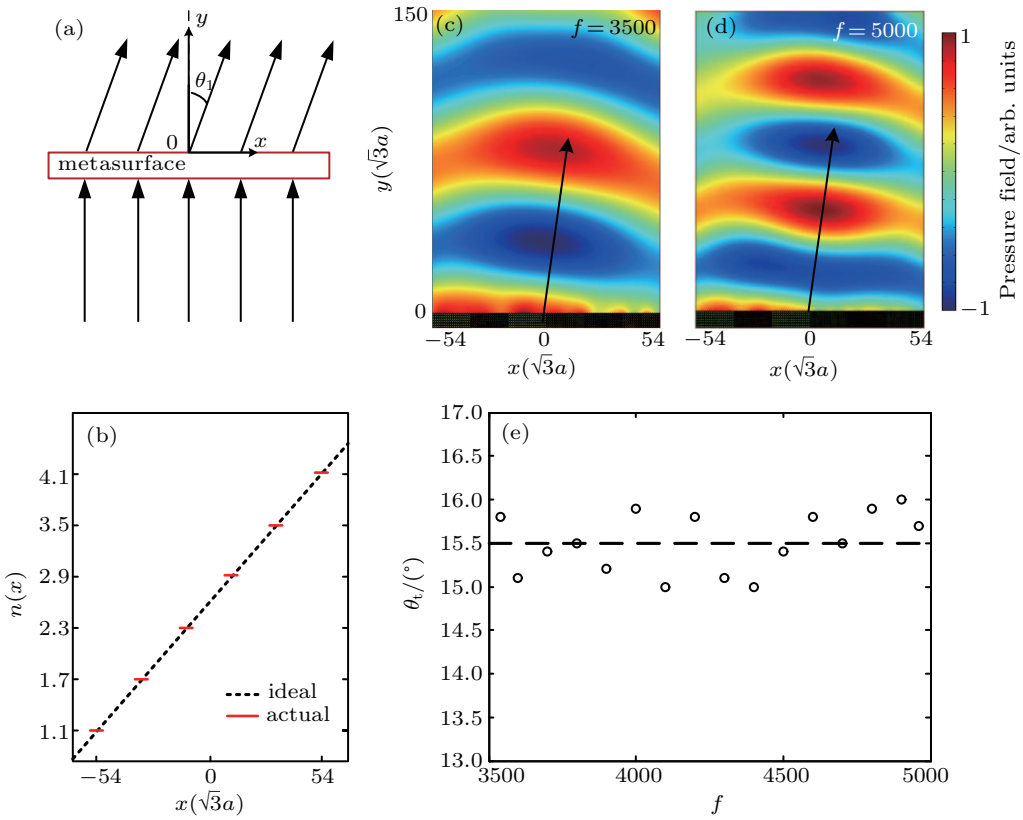


Fig. 3. (a) Conceptual schematics of the conversion process to generate an anomalous refraction; (b) refractive index distribution for the ideal metasurface (black dotted line) and gradient metasurface (red solid line) at working frequency; simulated acoustic pressure field distribution of anomalous refraction at $f = 3500$ Hz (c) and 5000 Hz (d); (e) relationship between refraction angle and incident acoustic frequency.

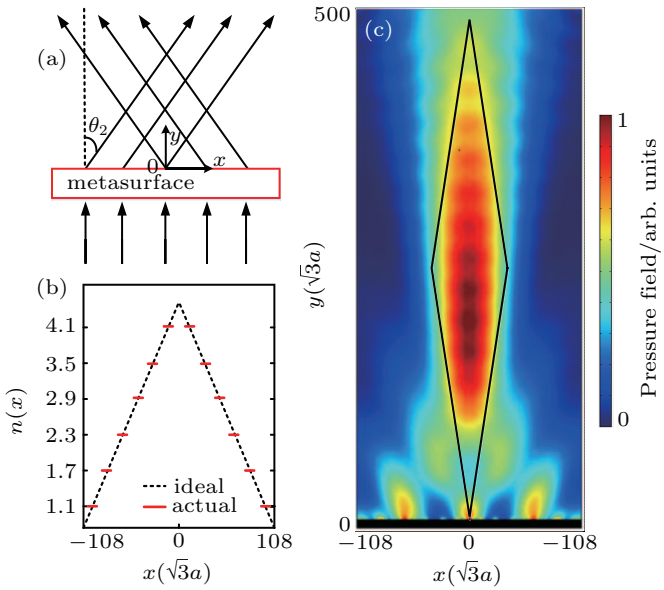


Fig. 4. (a) Conceptual schematic of the conversion process to generate a non-diffracting Bessel beam; (b) phase distribution for the ideal metasurface (black dotted line) and gradient metasurface (red solid line) at the working frequency; (c) simulated acoustic intensity field distribution of non-diffracting Bessel beam at $f = 5000$ Hz.

Figure 5(a) shows a conceptual schematic diagram of the acoustic focusing based on the metasurface. To achieve a focusing effect, it is necessary to enable all the transmitted acoustic rays to pass through the focus point. The focus point can be distributed on the axis or any other location. In this case, the focus position coordinate is assumed to be $(0, y_0)$. To concentrate the acoustic energy to the focus point, the refracted angle $\theta_t(x)$ of transmitted acoustic wave can be calculated from $\sin\theta_t(x) = -x/\sqrt{x^2+y_0^2}$. By substituting $\sin\theta_t(x)$ into Eq. (7), the refractive index profile of the ideal focused acoustic metasurface can be obtained from $n_3 = -\sqrt{x^2+y_0^2}/t_m + C_3$, where C_3 is an arbitrary constant. The black dashed line in Fig. 5(b) represents the refractive index distribution of the ideal metasurface along the x direction when $y_0 = 280a$ and $C_3 = 2413/100$. It can be found that the refractive index of the ideal metasurface is symmetrical and decreases as x increases. The discrete metasurface refractive index distribution is also shown in Fig. 5(b) (red solid line). In order to verify the focusing effect of the designed pentamode metasurface, the acoustic energy field distribution is calculated based on the FEM simulation. The black solid line in Fig. 5(c) is the intensity distribution in the horizontal direction of $y = y_0$ in Fig. 5(d). The normalized results show that the intensity at the focal point is about 1.7 times the incident intensity. Figure 5(d) illustrates the distribution of the acoustic energy field when a plane acoustic beam of frequency $f = 4000$ Hz is incident vertically on the pentamode metasurface. According to the reciprocity principle, this metasurface can also realize the conversion of cylindrical waves into plane waves. Figure 6(a) is a conceptual schematic diagram of waveform conversion.

When a cylindrical wave is incident on the pentamode metasurface, it emits the point source located at the focus position with frequency $f = 4000$ Hz. The acoustic pressure distribution field is shown in Fig. 6(b). It can be found that the cylindrical incident wave is converted into a plane wave after passing through the metasurface, realizing waveform conversion. The pentamode metasurface can also be considered as a broadband flat focusing lens with a sub-wavelength thickness.

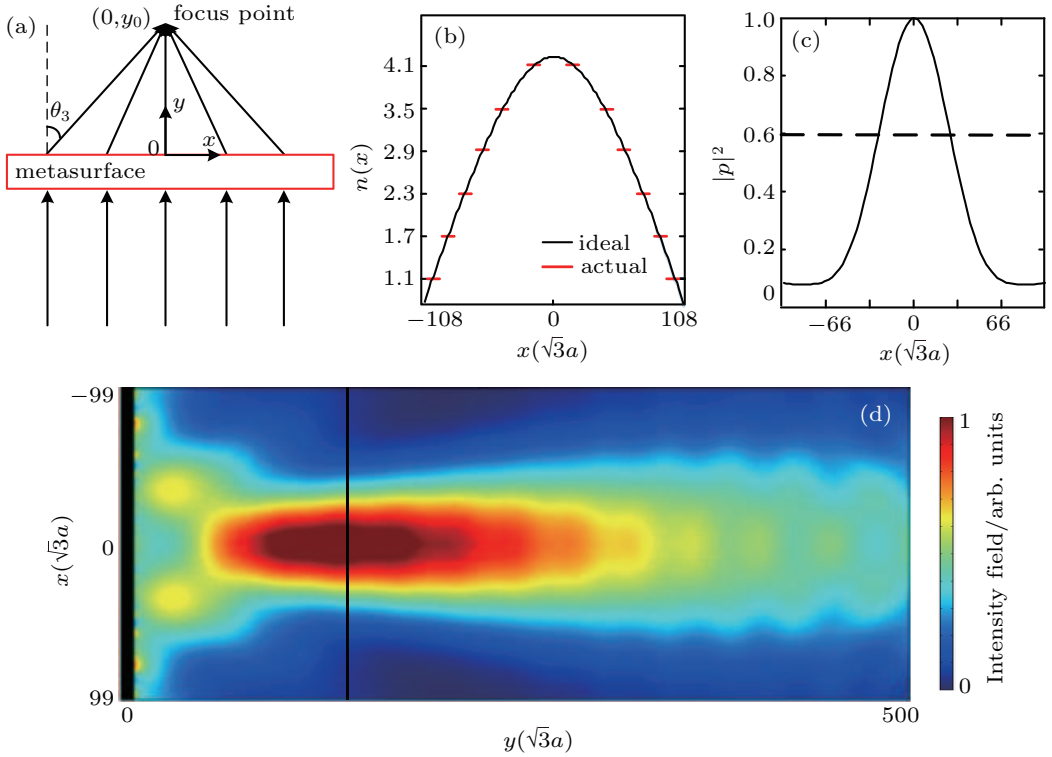


Fig. 5. (a) Conceptual schematic of conversion process of generating sub-wavelength flat focusing; (b) refractive index distribution for ideal metasurface (black solid line) and gradient metasurface (red solid line) at working frequency; (c) ideal and actual normalized transverse cross-sectional pressure intensity distribution along the y axis at the focal point; (d) simulated acoustic intensity field distribution of sub-wavelength flat focusing at $f = 4000$ Hz.

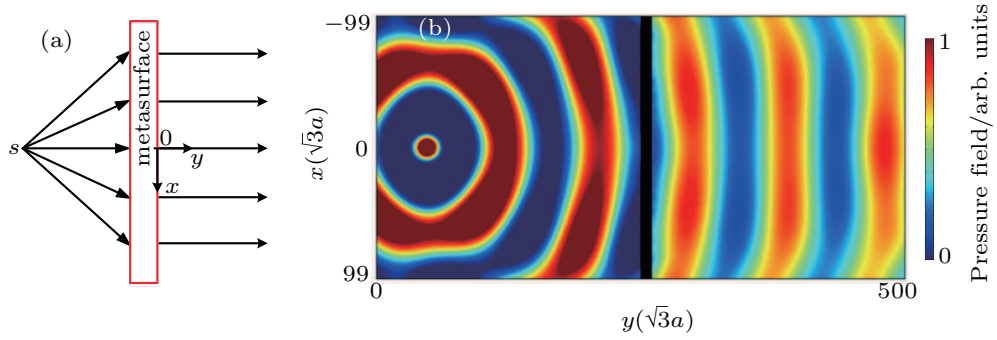


Fig. 6. (a) Conceptual schematic of the cylindrical-to-plane-wave conversion; (b) simulated acoustic pressure field distribution of cylindrical-to-plane-wave conversion beam at $f = 4000$ Hz.

4. Conclusions and perspectives

In this paper, the generalized acoustic Snell's law is extended to broadband and an impedance matching acoustic metasurface based on pentamode materials is proposed. The metasurface has a refractive index with a gradient distribution and its acoustic impedance matches with the background medium. According to the liquid-like elastic property of pentamode metamaterial, we design a series of non-dispersive pentamode material units with different refractive indices to construct acoustic metasurface with high transmission efficiency. Finally, broadband and high-efficiency acoustic wave anomalous refraction, Bessel beam generation, and acoustic focusing are all actualized based on the pentamode metasurface. The research work in this paper provides a new idea for wide-band and efficient acoustic wave modulation, and has potential application values in acoustic imaging, acoustic focusing, acoustic detection, and other fields.

Acknowledgment

The authors thank other people and groups for their making scientific contribution to this work.

References

[1] Yu N, Genevet P, Kats M A, Aieta F, Tetienne J P, Capasso F and Gaburro Z 2011 *Science* **334** 333
[2] Ni X, Emani N K, Kildishev A V, Boltasseva A and Shalaev V M 2012 *Science* **335** 427
[3] Sun S, He Q, Xiao S, Xu Q, Li X and Zhou L 2012 *Nat. Mater.* **11** 426
[4] Boltasseva A, Kildishev A V and Shalaev V M 2013 *Science* **339** 1232009
[5] Lin J, Mueller J P B, Wang Q, Yuan G, Antoniou N, Yuan X C and Capasso F 2013 *Science* **340** 331
[6] Kuester E F, Mohamed M A, Piket-May M and Holloway C L 2003 *IEEE Trans. Anten. Propag.* **51** 2641
[7] Li Y 2017 *Physics* **46** 721 (in Chinese)
[8] Ahmadi A, Ghadarghadr S and Mosallaei H 2010 *Opt. Express* **18** 123
[9] Memarzadeh B and Mosallaei H 2011 *Opt. Lett.* **36** 2569
[10] Tian Y, Wei Q, Cheng Y, Xu Z and Liu X 2015 *Appl. Phys. Lett.* **107** 333
[11] Díaz-Rubio A and Tretyakov S A 2017 *Phys. Rev. B* **96** 125409
[12] Zhu H and Semperlotti F 2016 *Phys. Rev. Lett.* **117** 034302
[13] Sun H X, Xin F, Yong G, Ren X D and Yuan S Q 2017 *Acta. Phys. Sin.* **66** 244301 (in Chinese)
[14] Su X, Norris A N, Cushing C W, Haberman M R and Wilson P S 2017 *J. Acoust. Soc. Am.* **141** 4408
[15] Li X C and Liu Z Y 2005 *Phys. Lett. A* **338** 413
[16] Khelif A, Choujaa A, Benchabane S, Djafarirouhani B and Laude V 2004 *Appl. Phys. Lett.* **84** 4400
[17] Sun Z, Jia H, Chen Y, Wang Z and Yang J 2018 *J. Acoust. Soc. Am.* **143** 1029
[18] Aieta F, Genevet P, Kats M A, Yu N, Blanchard R, Gaburro Z and Capasso F 2012 *Nano Lett.* **12** 4932
[19] Liang Z and Li J 2012 *Phys. Rev. Lett.* **108** 114301
[20] Xie Y, *Popa* B I, Zigoneanu L and Cummer S A 2013 *Phys. Rev. Lett.* **110** 175501
[21] Xie Y, Konneker A, Popa B I and Cummer S A 2013 *Appl. Phys. Lett.* **103** 201906
[22] Li Y F, Zhang J Q, Qu S B, Wang J F, Zheng L, Zhou H, Xu Z, Zhang A X 2015 *Chin. Phys. B* **24** 014202
[23] Milton G W and Cherkaev A V 1995 *J. Eng. Mater. Technol.* **117** 483
[24] Hladky-Hennio A C, Vasseur J O, Haw G, Croenne C, Haumesser L and Norris A N 2013 *Appl. Phys. Lett.* **102** 144103
[25] Layman C N, Naify C J, Martin T P, Calvo D C and Orris G J 2013 *Phys. Rev. Lett.* **111** 024302
[26] Bückmann T, Thiel M, Kadic M, Schittny R and Wegener M 2014 *Nat. Commun.* **5** 4130
[27] Chen Y, Liu X N, Xiang P and Hu G K 2016 *Adv. Mech.* **46** 382 (in Chinese)
[28] Norris A N and Nagy A J 2011 *First International Conference on Phonic Crystal, Metamaterials and Optomechanics*, May 29–June 2, 2011, Santa Fe, New Mexico, USA, p. 112
[29] Kadic M, Buckmann T, Schittny R, Gumbsch P and Wegener M 2014 *Phys. Rev. Appl.* **2** 054007
[30] Fokin V, Ambati M, Sun C and Zhang X 2007 *Phys. Rev. B* **76** 144302